

REGULAR OSCILLATIONS IN SYSTEMS WITH STOCHASTIC RESONANCE

GRIGORI N. MILSTEIN, MICHAEL V. TRETYAKOV

Weierstraß-Institut für Angewandte Analysis und Stochastik
Mohrenstr. 39, D-10117 Berlin , Germany
e-mail: milstein@wias-berlin.de

Department of Mathematics
Ural State University, Lenin str. 51, 620083 Ekaterinburg, Russia
e-mail: Michael.Tretyakov@usu.ru

1991 *Mathematics Subject Classification.* 60H10, 93E30.

Key words and phrases. Noise-driven monostable, bistable, and coupled bistable systems; periodic forcing; boundary value problems of parabolic type; numerical integration of stochastic differential equations.

ABSTRACT. Constructive sufficient conditions for regular oscillations in systems with stochastic resonance are given. For bistable systems, they rely on the fact that the probability of transition of a point from one well to the other with subsequent stay there during the half-period of the periodic forcing is close to 1. Using these conditions, domains of parameters corresponding to the regular oscillations are indicated. The regular oscillations are considered in bistable and monostable systems with additive and multiplicative noise. Special attention is paid to numerical methods. Algorithms based on numerical integration of stochastic differential equations turn out to be most natural both for simulation of sample trajectories and for solution of related boundary value problems of parabolic type. Results of numerical experiments are presented.

1991 Mathematics Subject Classification. 60H10, 93E30.

Key words and phrases. Noise-driven monostable, bistable, and coupled bistable systems; periodic forcing; boundary value problems of parabolic type; numerical integration of stochastic differential equations.

1. Introduction

One of the remarkable properties of a noise-driven bistable system subject to small deterministic periodic perturbations is the existence of regular oscillations under a certain set of parameters of the system. The oscillations are connected with the phenomenon of amplifying the response to a small periodic forcing which is commonly referred as stochastic resonance (SR). SR was first considered in the context of a model concerning climate dynamics [2, 22]. In these initial works a fairly simple and robust mechanism of regular oscillations was explained. Then SR has been observed in a large variety of systems including lasers, noise-driven electronic circuits, superconducting quantum interference devices, chemical reactions, etc. Some theoretical investigations of SR have been done as well. SR is also simulated numerically for various physical and neurobiological problems modelled by stochastic differential equations (SDE). For a review and extended list of references on SR see, e.g. [6, 14, 20, 24].

Some conditions for regular oscillations, based on Kramers' theory of diffusion over a potential barrier, are introduced in [2]. The subject of our paper is to give new constructive sufficient conditions for the presence of regular oscillations. Using these conditions, we indicate domains of parameters under which regular oscillations exist.

A typical system, for which the SR phenomenon is observed, has the form of the Ito equation

$$dX = a(X)dt + b(t)dt + \sigma(t, X)dw(t), \quad (1.1)$$

where b and σ are periodic in t , $w(t)$ is a standard Wiener process.

For instance, the system

$$dX = (\alpha X - X^3)dt + A \cos \nu t dt + \sigma dw(t) \quad (1.2)$$

has the form (1.1).

The following system in the sense of Stratonovich [1]

$$dX = (\alpha - X - 2c \frac{X}{1 + X^2})dt + A \cos \nu t dt + \sigma \frac{X}{1 + X^2} * dw(t) \quad (1.3)$$

can be presented in the form (1.1) as well.

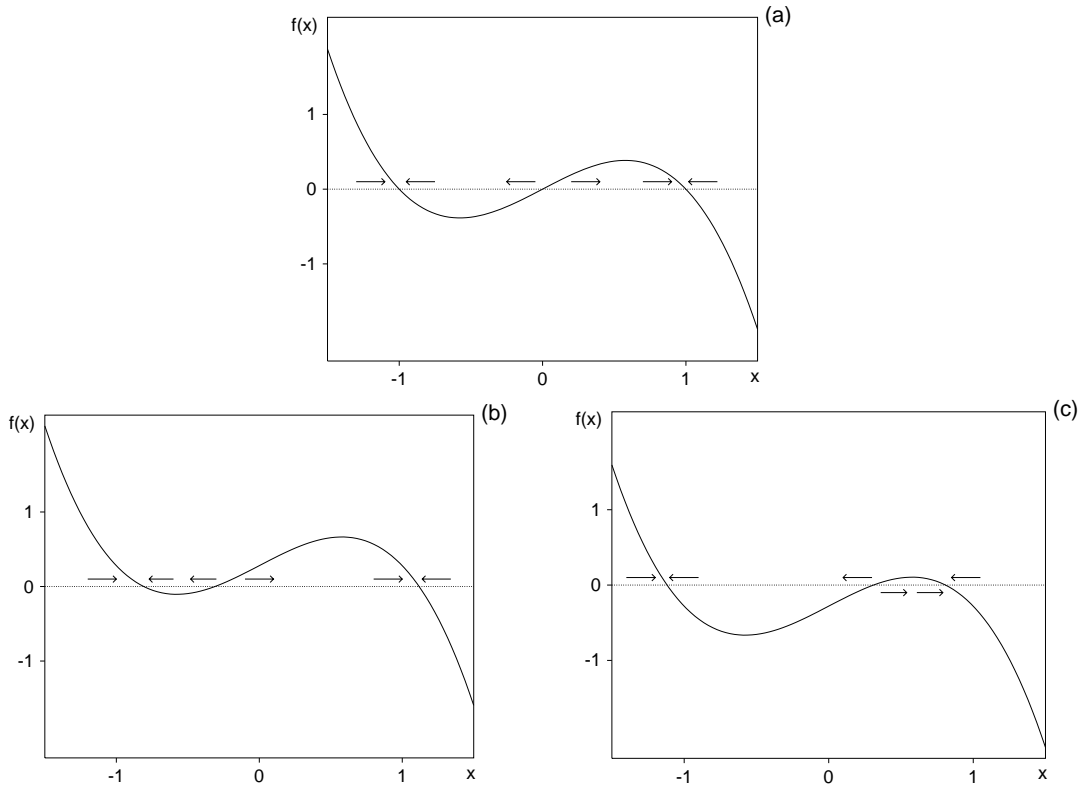


FIGURE 1.1. The function $f(x) = x - x^3 + A$ under (a) $A = 0$, (b) $A = 0.28$, and (c) $A = -0.28$.

We prefer to investigate the conditions of arising regular oscillations for a specific system which is similar to (1.2) [2]:

$$dX = (X - X^3)dt + A\chi(t; \theta)dt + \sigma dw(t), \quad (1.4)$$

where $\chi(t; \theta)$ is the following θ -periodic function:

$$\chi(t; \theta) = \begin{cases} 1, & 0 \leq t < \frac{\theta}{2}, \\ -1, & \frac{\theta}{2} \leq t < \theta. \end{cases} \quad (1.5)$$

Thus, θ is a period and A is an amplitude of the constraining oscillations.

The mechanism of arising regular oscillations is described in [2] (see [6, 14, 20, 24] as well). For clarity of exposition, let us give an explanation of the mechanism. It differs from [2] in form only. In absence of the noise ($\sigma = 0$) and the periodic forcing ($A = 0$) equation (1.4) has the stationary points $x = -1$, $x = 0$, $x = 1$. The points $x = -1$ and $x = 1$ are stable and $x = 0$ is unstable (see Figure 1.1a, where $f(x)$ is the right side of the equation (1.4) under $\sigma = 0$, $A = 0$). Under $\sigma = 0$ and not large $A > 0$ the stationary points are displaced as shown in Figure 1.1b during the first half-period and as in Figure 1.1c during the second half-period. Clearly, under $\sigma = 0$ a point from a neighborhood of $x = -1$ (from the left well) cannot get into a neighborhood of $x = 1$ (into the right well) and conversely. Such transitions become possible under $\sigma \neq 0$. If (for some parameters A , θ , σ) a point from the left well attains the point $x = 1$ with probability close to 1 at a random time $s < \theta/2$ and

after that it remains in the right well during the time $\theta/2 - s$ with the probability close to 1, then regular transitions (regular oscillations) arise. Indeed, after the half-period the system acts by virtue of Figure 1.1c and due to the symmetry the situation repeats with changing the left well for the right one.

In Section 2 we investigate two probabilities in conjunction with Figure 1.1b: the probability of attainability of the point $x = 1$ from $x = -1$ for a time less than $\theta/2$ (which can be considered as the probability of getting into the right well from the left one) and the probability of unattainability of the point $x = 0$ from $x = 1$ during the half-period $\theta/2$. It is clear that the closeness of the product p of the probabilities to 1 is a sufficient condition for the presence of regular oscillations. We observe that at the same time some fluctuations of such a regular behavior are unavoidable: it always remains a positive probability of unattainability from the left well into the right one; sometimes more than two transitions may occur during one period and so on. In other words, we assign a probability to the very phenomenon of regular oscillations and the above-mentioned product p bounds this probability from below. The magnitude of p is found in Section 2 by numerical solution of two boundary value problems of parabolic type. As a result, given a level of probability, a domain of the parameters can be found such that the probability of regular oscillations is above this level. The approach proposed here and the approach based on Kramers' theory of diffusion over a potential barrier are compared in Section 3. In Section 4 we consider a system of the form (1.4) with σ depending on t, X (or on X only). Due to the multiplicative noise, one can essentially extend the domain of parameters A, θ, σ guaranteeing regular oscillations. Particularly, we succeed to get high-frequency regular oscillations. Section 5 deals with large-amplitude regular oscillations in a monostable system. In Section 6 a system of two coupled oscillators is considered. An increase of coupling leads to shift of the domain of parameters corresponding to the regular oscillations. Special attention is paid to numerical methods. Algorithms based on numerical integration of stochastic differential equations turn out to be most natural both for simulation of sample trajectories and for solution of arising boundary value problems of parabolic type. Numerical algorithms used in the experiments are presented in the Appendix.

2. The sufficient conditions for regular oscillations

Let $X_{s,x}(t)$ be the solution of (1.4) which starts from the point x at the moment s . If $s = 0$, we write $X_x(t)$ instead of $X_{0,x}(t)$. It is known [2] that for suitable A, θ, σ a point from a neighborhood of the point $x = -1$ gets into a neighborhood of the point $x = 1$ during the half-period $\theta/2$ with the probability close to 1 and remains there up to the end of the half-period. The same takes place in the time interval $[\theta/2, \theta)$ in reverse order. Then all the events are repeated.

Let us underline: under the regular oscillations we understand a behavior of the solution $X(t)$ such that $X_{-1}(t)$ reaches $x = 1$ at a time moment τ less than $\theta/2$ and $X_{\tau,1}(t)$ remains greater than zero during the rest of the half-period. Namely for this phenomenon, we assign a probability $p_{ro}(A, \theta, \sigma)$ (probability of regular oscillations). For instance, due to our notion, the regular oscillations presented on Figure 2.4c correspond to the probability ≈ 0.8 ($X_{\tau,1}(t)$ reaches $x = 0$ two times per 10 periods on average).

As it has been explained in Introduction, acceptable sufficient conditions of the regular oscillations are the following ones:

the probability

$$p_{-1,1} = p_{-1,1}(A, \theta, \sigma) := P(X_{-1}(t) < 1, 0 \leq t \leq \frac{\theta}{2}) \quad (2.1)$$

has to be small, and

the probability

$$p_{1,0} = p_{1,0}(A, \theta, \sigma) := P(X_1(t) > 0, 0 \leq t \leq \frac{\theta}{2}) \quad (2.2)$$

has to be close to 1.

It is clear as well that the regular oscillations will occur with the probability p_{ro} which exceeds the product

$$p = p(A, \theta, \sigma) := q_{-1,1}(A, \theta, \sigma) \cdot p_{1,0}(A, \theta, \sigma), \quad (2.3)$$

where $q_{-1,1} = 1 - p_{-1,1}$.

So, we conclude that

(RO) *The closeness of $p = p(A, \theta, \sigma)$ to 1 is a sufficient condition of regular oscillations.*

Clearly, the condition of closeness of the probability $q_{-1,1}(\sigma, A, \theta)$ to 1 is necessary, but closeness of $p_{1,0}(A, \theta, \sigma)$ to 1 is not necessary for the regular oscillations. Indeed, $X_{-1}(t)$ reaches $x = 1$ after some time $\tau > 0$ and in fact we need that $X_{\tau,1}(t)$ remains in the neighborhood of $x = 1$ during a time less than $\theta/2$.

Let us find the probability $p_{ro}(A, \theta, \sigma)$. Denote the first-passage time of $X_{-1}(t)$ to $x = 1$ as $\tau_{-1}(1)$ and the first-passage time of $X_1(t)$ to $x = 0$ as $\tau_1(0)$. Consider the probabilities $p_1(t; A, \sigma) := P(\tau_{-1}(1) \leq t)$ and $p_2(t; A, \sigma) := P(\tau_1(0) > t)$. Note that $p_1(\theta/2; A, \sigma) = q_{-1,1}(A, \theta, \sigma)$ and $p_2(\theta/2; A, \sigma) = p_{1,0}(A, \theta, \sigma)$. Introduce the equidistant time discretization of the interval $\theta/2 : t_j = j \cdot h, j = 0, \dots, N, h = \theta/(2N)$. It is evident that

$$\begin{aligned} & \sum_{j=0}^{N-1} P(\tau_{-1}(1) \in [t_j, t_{j+1})) P(\tau_1(0) > \theta/2 - t_{j+1}) \geq p_{ro} \\ & \geq \sum_{j=0}^{N-1} P(\tau_{-1}(1) \in [t_j, t_{j+1})) P(\tau_1(0) > \theta/2 - t_j) \end{aligned}$$

and

$$P(\tau_{-1}(1) \in [t_j, t_{j+1})) = p_1(t_{j+1}; A, \sigma) - p_1(t_j; A, \sigma).$$

Hence we get

$$p_{ro}(A, \theta, \sigma) = \int_0^{\theta/2} p_1'(t; A, \sigma) p_2(\theta/2 - t; A, \sigma) dt, \quad p_1' = \frac{dp_1}{dt}. \quad (2.4)$$

One can see that $p(A, \theta, \sigma) \leq p_{ro}(A, \theta, \sigma) \leq q_{-1,1}(A, \theta, \sigma)$. Closeness of p_{ro} to 1 gives the necessary and sufficient condition of the regular oscillations. But this condition is less constructive than the given above sufficient condition (RO). Besides, the product p from (2.3) approximates p_{ro} quite good according to our numerical experiments.

Our urgent aim is to evaluate $p(A, \theta, \sigma)$. To this end introduce the functions

$$u(s, x) = u(s, x; A, \theta, \sigma) := 1 - P(X_{s,x}(t) < 1, s \leq t \leq \frac{\theta}{2}), \quad 0 \leq s \leq \frac{\theta}{2}, \quad x \leq 1, \quad (2.5)$$

and

$$v(s, x) = v(s, x; A, \theta, \sigma) := P(X_{s,x}(t) > 0, s \leq t \leq \frac{\theta}{2}), \quad 0 \leq s \leq \frac{\theta}{2}, \quad x \geq 0. \quad (2.6)$$

We get

$$1 - p_{-1,1} = u(0, -1), \quad p_{1,0} = v(0, 1), \quad p = u(0, -1) \cdot v(0, 1). \quad (2.7)$$

Clearly,

$$u(s, x) = 1 - P(X_{s,x}(t) < 1, s \leq t \leq \frac{\theta}{2}) = 1 - E\varphi(X_{s,x}(\tau_{s,x} \wedge \frac{\theta}{2})), \quad (2.8)$$

where $\tau_{s,x} = \tau_{s,x}(1)$ is the first (random) moment at which $X_{s,x}(t) = 1$ and

$$\varphi(x) = \begin{cases} 1, & x < 1, \\ 0, & x = 1. \end{cases}$$

Therefore (see, e.g., [5]), the function $u(s, x)$ satisfies the following parabolic equation in half-band:

$$\frac{\partial u}{\partial s} + \frac{1}{2}\sigma^2 \frac{\partial^2 u}{\partial x^2} + (x - x^3 + A) \frac{\partial u}{\partial x} = 0, \quad 0 \leq s < \frac{\theta}{2}, \quad x < 1, \quad (2.9)$$

with the initial and boundary conditions:

$$\begin{aligned} u(\frac{\theta}{2}, x) &= 0, \quad x < 1, \\ u(s, 1) &= 1, \quad 0 \leq s \leq \frac{\theta}{2}. \end{aligned} \quad (2.10)$$

Analogously,

$$v(s, x) = P(X_{s,x}(t) > 0, s \leq t \leq \frac{\theta}{2}) = E\psi(X_{s,x}(\theta_{s,x} \wedge \frac{\theta}{2})), \quad (2.11)$$

where $\theta_{s,x} = \tau_{s,x}(0)$ is the first (random) moment at which $X_{s,x}(t) = 0$ and

$$\psi(x) = \begin{cases} 1, & x > 0, \\ 0, & x = 0. \end{cases}$$

The function $v(s, x)$ satisfies the following parabolic boundary value problem in half-band:

$$\frac{\partial v}{\partial s} + \frac{1}{2}\sigma^2 \frac{\partial^2 v}{\partial x^2} + (x - x^3 + A) \frac{\partial v}{\partial x} = 0, \quad 0 \leq s < \frac{\theta}{2}, \quad x > 0, \quad (2.12)$$

$$\begin{aligned} v(\frac{\theta}{2}, x) &= 1, \quad x > 0, \\ v(s, 0) &= 0, \quad 0 \leq s \leq \frac{\theta}{2}. \end{aligned} \quad (2.13)$$

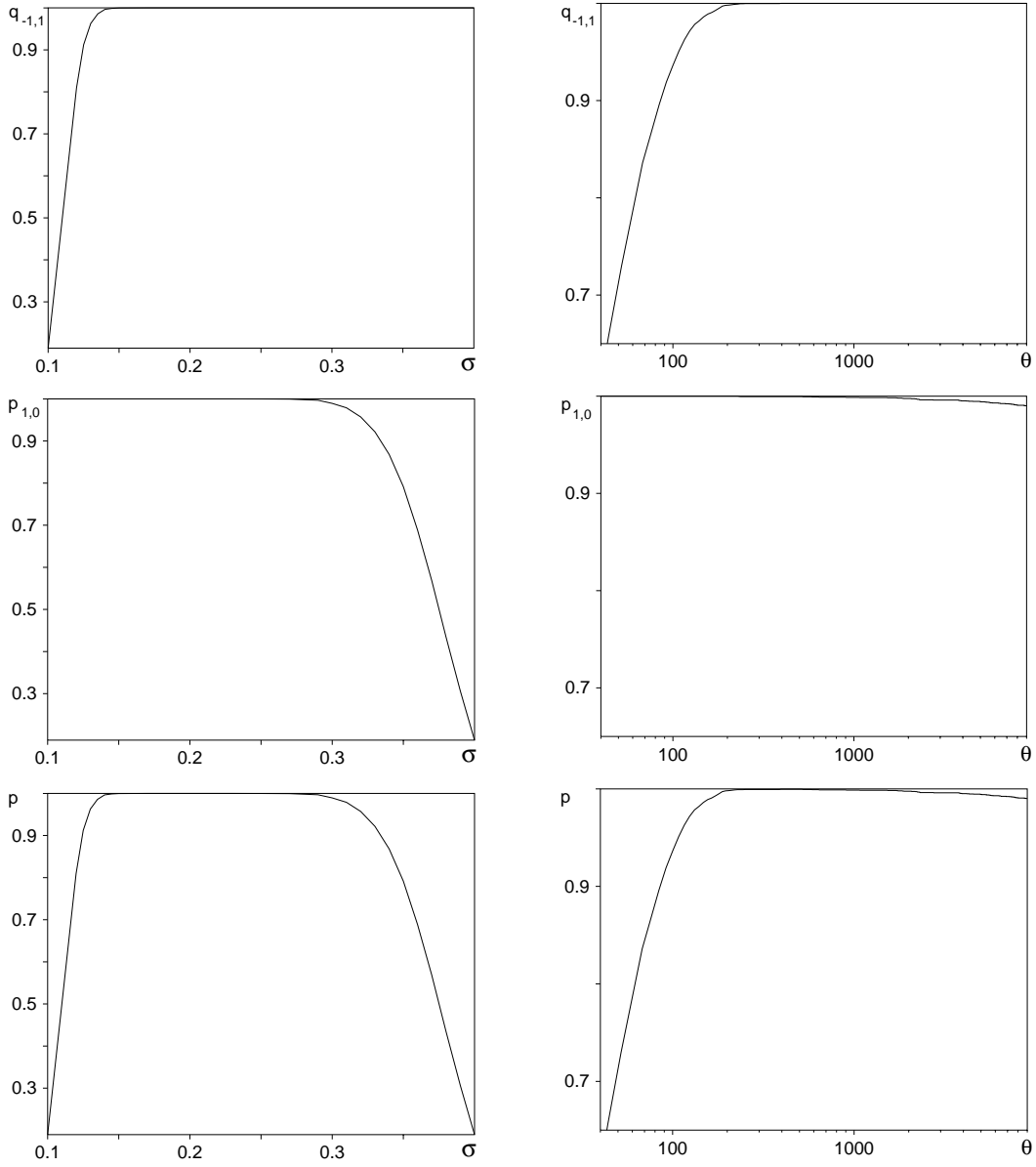


FIGURE 2.1. Dependence of the probabilities $q_{-1,1}(A, \sigma, \theta)$ and $p_{1,0}(A, \sigma, \theta)$ and the product $p(A, \sigma, \theta)$ in σ under $A = 0.28$, $\theta = 10^4/3$ (left column) and in θ under $A = 0.28$, $\sigma = 0.29$ (right column, with log scaling in θ).

Remark 2.1. It is easy to formulate sufficient conditions and the corresponding boundary value problems in the case of another system, for instance, for the system (1.2).

It is not difficult to prove that the function $u(s, x; A, \theta, \sigma)$ is increasing and the function $v(s, x; A, \theta, \sigma)$ is decreasing with respect to θ . Therefore, there is a range of $\theta \in (\theta_*(A, \sigma), \theta^*(A, \sigma))$, where under fixed A and σ the product $p(A, \theta, \sigma)$ reaches its maximum. Analogously, in a range of the noise intensity $\sigma \in (\sigma_*(A, \theta), \sigma^*(A, \theta))$, the product $p(A, \theta, \sigma)$ reaches its maximum under fixed A and θ . We take the amplitude of the constraining oscillations less than $A^* = 2\sqrt{3}/9$ so that the system (1.4) has

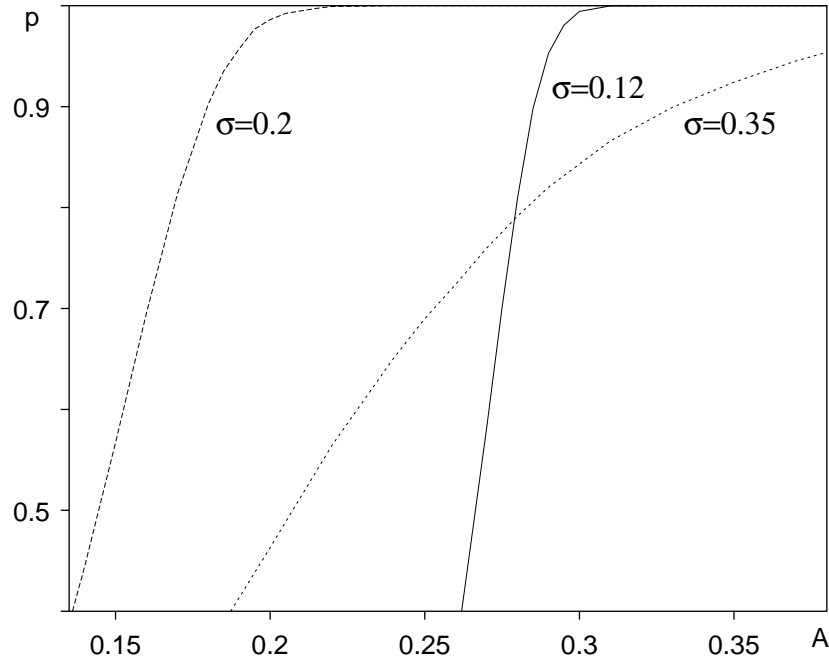


FIGURE 2.2. Dependence of the product $p(A, \sigma, \theta)$ in A under $\theta = 10^4/3$ and various σ .

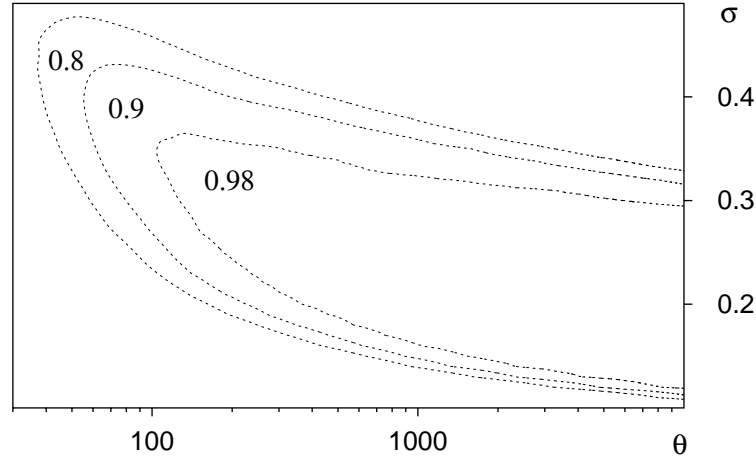


FIGURE 2.3. Level curves of the product $p(A, \sigma, \theta)$ in the plane (θ, σ) under $A = 0.28$; θ in the logarithmic scale.

three stationary points under $A < A^*$ and $\sigma = 0$. Evidently, the product $p(A, \theta, \sigma)$ is an increasing function with respect to A under fixed θ and σ .

As is known and has already been mentioned, there is a domain of parameters such that the regular oscillations are observed. Due to the sufficient condition of

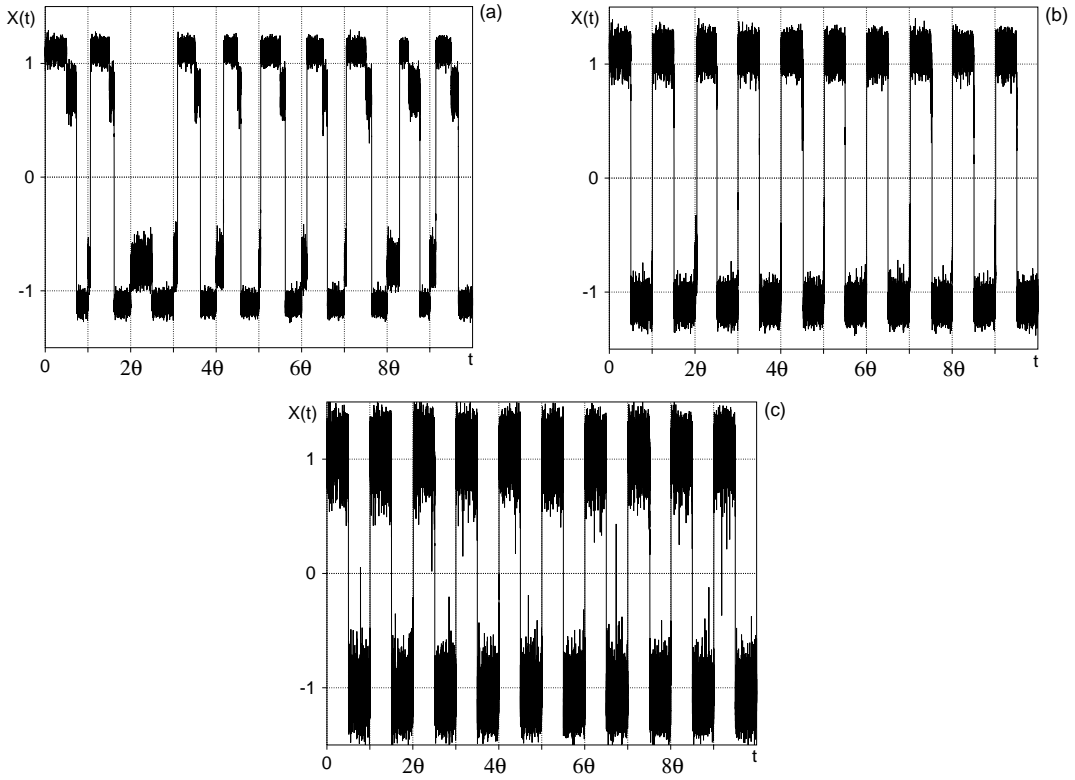


FIGURE 2.4. Sample trajectories of the solution to (1.4) under $A = 0.28$, $\theta = 10^4/3$, and various σ : (a) $\sigma = 0.12$, (b) $\sigma = 0.2$, and (c) $\sigma = 0.35$.

regular oscillations (RO), we are able to get estimates of this domain from below in terms of the product $p(A, \theta, \sigma)$.

To find the probabilities $q_{-1,1}$ and $p_{1,0}$, we have to solve the problems (2.9)-(2.10) and (2.12)-(2.13) numerically. In a number of tests we have used both finite-difference schemes and probability methods from [16] and have seen ourselves that they give coincident results. Due to the fact that the absolute value of the term $x - x^3$ becomes big at $|x| \gg 1$, there are difficulties in implementation of finite-difference schemes for solving the boundary value problems (2.9)-(2.10) and (2.12)-(2.13). The difficulties do not arise in simulating the problems by the probabilistic methods. Moreover, we need in the individual values $u(0, -1)$, $v(0, 1)$ only and in such a case the probabilistic approach with the Monte Carlo technique is most relevant. That is why we mainly use the probabilistic methods in our experiments and attract finite-difference ones from time to time to control the obtained results. See a description of one of the used probabilistic methods in Appendix.

Let us give some illustrations now. Figures 2.1 and 2.2 show typical behavior of the probabilities $q_{-1,1}(\sigma, A, \theta)$ and $p_{1,0}(\sigma, A, \theta)$ and of the product $p(\sigma, A, \theta)$. The remarkable feature is that there is a range of parameters where the product p is close to 1 that corresponds to the regular oscillations. Given the level of the product p , the domains of parameters are indicated on Figure 2.3. Let us emphasize that the range of parameters for the regular oscillations is fairly large.

Figure 2.4 presents sample trajectories of the solution to SDE (1.4). We take values of parameters corresponding to Figure 2.1. For the parameters σ, A, θ such

that the product $p(\sigma, A, \theta)$ is close to 1, i.e., the sufficient condition (RO) takes place, we observe the regular oscillations (see Figure 2.4b). A sample trajectory in the case when $q_{-1,1} \approx 0.8$ and $p_{1,0} \approx 1$, i.e., when the necessary condition does not fulfill, is given on Figure 2.4a. One can see that transitions between two wells during $\theta/2$ occur with the probability close to 0.8. Figure 2.4c demonstrates a typical trajectory in the case of $q_{-1,1} \approx 1$ and $p_{1,0} \approx 0.8$. After reaching $x = 1$ ($x = -1$), the trajectory remains in the corresponding well during the rest of the half-period with the probability close to 0.8. To simulate trajectories, we use the mean-square Euler method (see Appendix for details).

Remark 2.2. The proposed here approach can also be carried over to the problem of noise-induced transport in Brownian ratchets [12] (for a review on this topic see, e.g. [8, 10, 13]). The noisy periodically-driven overdamped ratchets dynamics is usually described by the Ito equation

$$dX = a(X)dt + b(t)dt + \sigma dw(t),$$

where $F(x) = \int a(x)dx$ is an L -periodic ratchet potential $F(x) = F(x + L)$, $x \in R^1$, possessing no reflection symmetry $F(x) \neq F(-x)$, $x \in (0, L/2)$, $b(t)$ is a θ -periodic function, and $w(t)$ is a standard Wiener process.

A noise-induced directed current is observed in such a system with small periodic forcing under some set of parameters. By our approach we are able to assign a probability and to give constructive sufficient conditions for this phenomenon. A separate paper will be devoted to this subject.

3. Comparison with the approach based on Kramers' theory of diffusion over a potential barrier

Without loss of generality (due to the symmetry) let us consider the system (1.4), when it acts by virtue of Figure 1.1b, i.e.,

$$dX = a(X)dt + \sigma dw(t), \quad a(x) = x - x^3 + A, \quad (3.1)$$

under $A < 2\sqrt{3}/9$.

Let us evaluate some mean characteristics of the random times $\tau_{-1}(1)$ and $\tau_1(0)$ introduced in the previous section (recall that $\tau_{-1}(1)$ is the first-passage time of $X_{-1}(t)$ to $x = 1$ and $\tau_1(0)$ is the first-passage time of $X_1(t)$ to $x = 0$).

The mean value $E\tau_{-1}(1)$ can be found in the following way. Consider the boundary value problem

$$\frac{1}{2}\sigma^2\psi'' + a(x)\psi' + 1 = 0, \quad \psi(C; C) = 0, \quad \psi(1; C) = 0, \quad C < -1,$$

for the function $\psi(x; C)$, where C is a parameter.

It is known [5, 7] that $\psi(-1; C)$ is equal to the mean value of the first-exit time of the process $X_{-1}(t)$ from the interval $(C, 1)$. Clearly, $E\tau_{-1}(1) = \lim_{C \rightarrow -\infty} \psi(-1; C)$, and also $E\tau_{-1}(1) = \Psi(-1)$, where $\Psi(x)$ is the solution to the problem

$$\frac{1}{2}\sigma^2\Psi'' + a(x)\Psi' + 1 = 0, \quad \Psi'(-\infty) = 0, \quad \Psi(1) = 0. \quad (3.2)$$

The mean $E\tau_1(0)$ can be found analogously.

The second moment $E\tau_{-1}^2(1)$ is equal to $\Psi_1(-1)$, where $\Psi_1(x)$ is the solution to the problem

$$\frac{1}{2}\sigma^2\Psi_1'' + a(x)\Psi_1' + 2\Psi(x) = 0, \quad \Psi_1'(-\infty) = 0, \quad \Psi_1(1) = 0,$$

and $\Psi(x)$ is the solution of the problem (3.2) (see [5, 7]).

The approach based on Kramers' theory employs the following conditions as sufficient ones for existence of regular oscillations (see, e.g., [2]; from principal point of view our exposition in this section only slightly differs from [2]):

- (i) $E\tau_{-1}(1) \ll \theta/2$,
- (ii) $E\tau_1(0) \gg \theta/2$,
- (iii) $(D\tau_{-1}(1))^{1/2} = [E\tau_{-1}^2(1) - (E\tau_{-1}(1))^2]^{1/2} \ll \theta/2$.

These conditions are fairly constructive because all the magnitudes $E\tau_{-1}(1)$, $E\tau_1(0)$, and $E\tau_{-1}^2(1)$ can be found by quadratures. Moreover, under small σ they can be expressed by exponential Kramers formulas.

In the previous section we propose an alternative approach, which is sufficiently constructive as well. Besides, one can get the more exhaustive answers using the sufficient condition (RO) from Section 2 in comparison with the conditions (i)-(iii) which are only qualitative in nature. Let us emphasize once more that in Section 2 the probability is assigned to the very phenomenon of regular oscillations.

4. High-frequency regular oscillations in systems with multiplicative noise

In the case of system (1.4) it is impossible to get high-frequency regular oscillations. Indeed, if we decrease the period length θ , we should increase the noise level σ to preserve the level of $q_{-1,1}$. But the probability $p_{1,0}$ decreases with an increase of σ . Therefore, the product p becomes low and regular oscillations disappear. In this section we consider systems with multiplicative noise such that the probability $p_{1,0}$ is always equal to 1 and due to this fact we shall be able to obtain high-frequency regular oscillations.

Consider the model with multiplicative time-dependent noise

$$dX = (X - X^3)dt + A\chi(t; \theta)dt + \sigma\gamma(t, X; \theta)dw(t), \quad (4.1)$$

where $\chi(t; \theta)$ is the θ -periodic function defined in (1.5) and $\gamma(t, x; \theta)$ is the following θ -periodic function

$$\gamma(t, x; \theta) = \begin{cases} 1, & 0 \leq t < \theta/2, \quad x < 1, \\ 0, & 0 \leq t < \theta/2, \quad x \geq 1, \\ 1, & \theta/2 \leq t < \theta, \quad x > -1, \\ 0, & \theta/2 \leq t < \theta, \quad x \leq -1. \end{cases} \quad (4.2)$$

As it was marked in [3] (where SR for periodically modulated noise intensity was considered), periodically modulated noise is not uncommon and it arises, for example, at the output of any amplifier whose gain varies periodically in time.

It is evident that in the case of (4.1)-(4.2) $p_{1,0} = 1$ and, consequently, the necessary and sufficient condition for regular oscillations consists in the closeness of the probability $q_{-1,1}(\sigma, A, \theta)$ to 1. This probability can be close to 1 even for a fairly

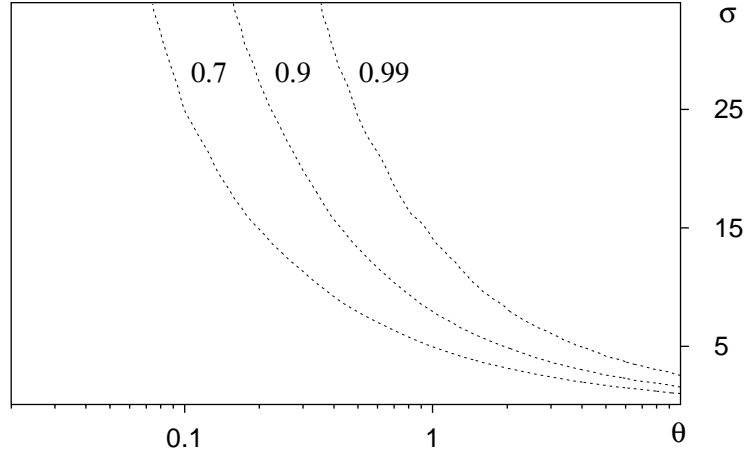


FIGURE 4.1. Level curves of the probability $q_{-1,1}(A, \sigma, \theta)$ in the plane (θ, σ) under $A = 0.28$; θ in the logarithmic scale.

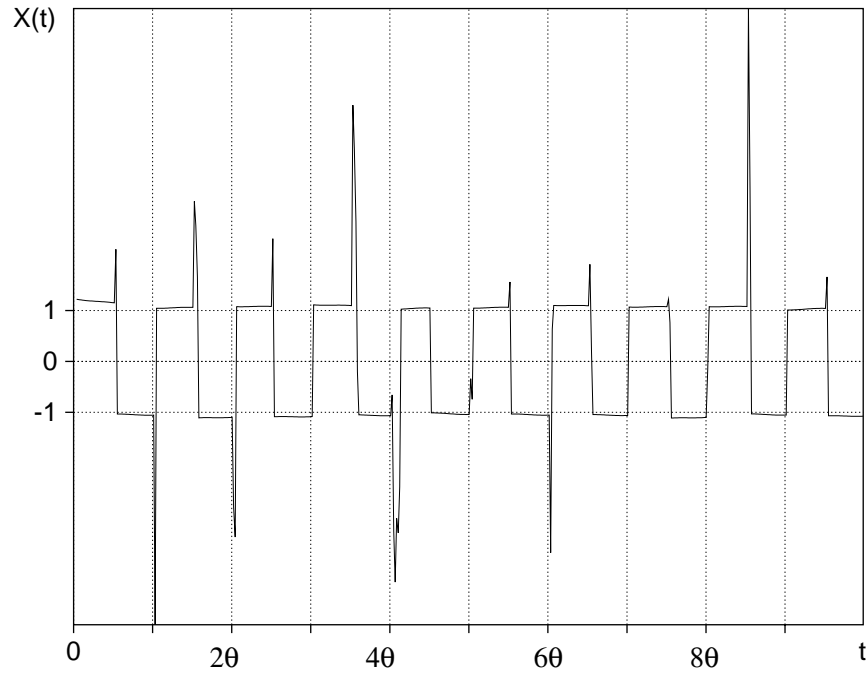


FIGURE 4.2. Sample trajectory of the solution to (4.1)-(4.2) under $\sigma = 35$, $A = 0.28$, $\theta = 2\pi/\nu \approx 0.524$ ($\nu = 12$).

small θ (i.e., for higher frequency $\nu = 2\pi/\theta$) and for very small A under an appropriate value of σ . Thus, it is possible to organize the high-frequency regular oscillations in the system (4.1)-(4.2) with small periodic forcing.

Figure 4.1 demonstrates level lines of $q_{-1,1}(\sigma, A, \theta)$ in the plane (σ, θ) under $A = 0.28$. A typical trajectory with the high-frequency oscillations is given on Figure

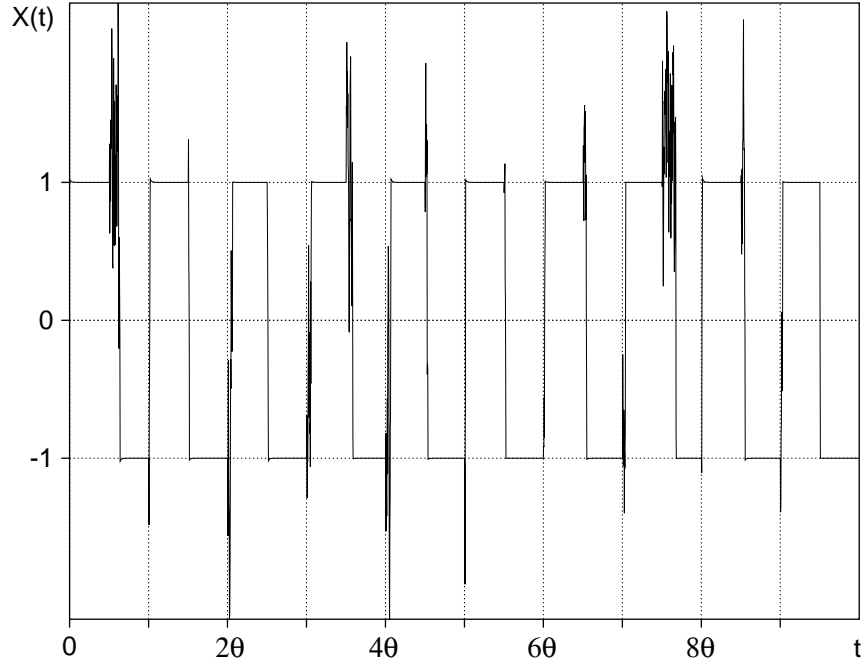


FIGURE 4.3. Sample trajectory of the solution to (4.1)-(4.2) under $\sigma = 2$, $A = 0$, $\theta = 2\pi/\nu \approx 31.42$ ($\nu = 0.2$).

4.2. In the case of the model (4.1)-(4.2) regular oscillations can be obtained under zero A (see Figure 4.3). Another system with high-frequency stochastic resonance was considered in [4].

Now consider the model with multiplicative time-independent noise

$$dX = (X - X^3)dt + A\chi(t; \theta)dt + \sigma\gamma(X)dw(t), \quad (4.3)$$

where

$$\gamma(x) = \begin{cases} 1, & -1 < x < 1, \\ 0, & \text{otherwise.} \end{cases} \quad (4.4)$$

Let the solution $X(t)$ to (4.3)-(4.4) start from $x = -1$. During the time $[0, \theta/2)$ the drift in the system (4.3) corresponds to Figure 1.1b. Clearly, the probability of attainability of the point $x = 1$ for the time less than $\theta/2$ is not less than $q_{-1,1}$ in the model (1.4)-(1.5). After reaching the point $x = 1$, the trajectory moves deterministically in positive direction to a point $X(\theta/2) > 1$. Then the drift in the system (4.3) becomes corresponding to Figure 1.1c and the trajectory changes its movement direction. The trajectory comes back to the point $x = 1$ at a moment $\theta/2 + \tau$, where τ is random. It remains the time $\theta/2 - \tau$ for the trajectory to reach the point $x = -1$.

The random moment τ is less than s^* which can be evaluated in the following way.

Let the solution $X(t)$ of the equation

$$X' = X - X^3 + A\chi(t; \theta)$$

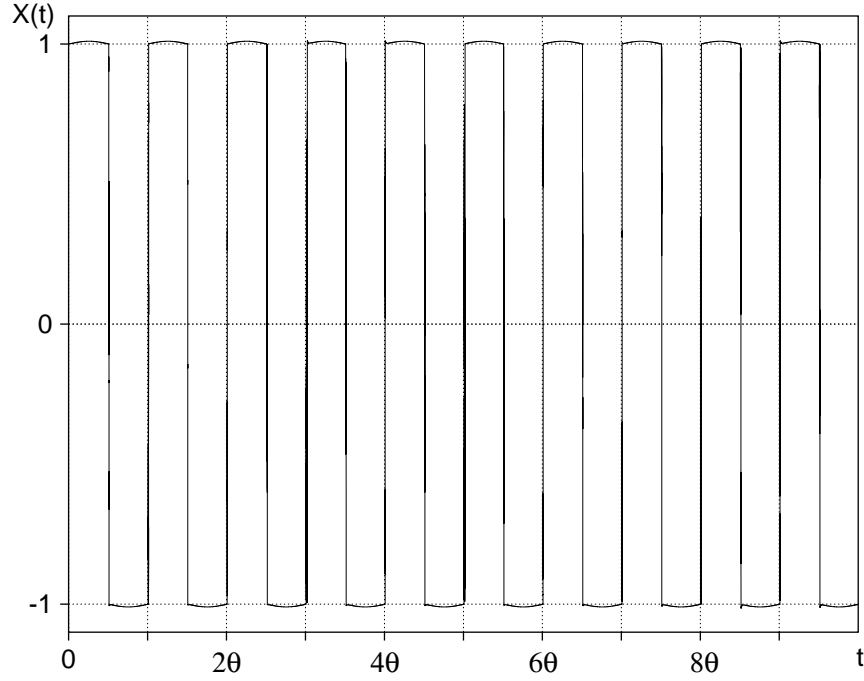


FIGURE 4.4. Sample trajectory of the solution to (4.3)-(4.4) under $\sigma = 3$, $A = 0.02$, $\theta = 2\pi/\nu \approx 62.83$ ($\nu = 0.1$).

start from $x = 1$. Then the trajectory $X(t)$ moves in positive direction up to $t = \theta/2$, when the trajectory changes its movement direction, and comes back to the point $x = 1$ at the instance $t^* \in (\theta/2, \theta)$. The value of the desired s^* is equal to $t^* - \theta/2$.

Introduce the probability

$$p_{-1,1}^* = p_{1,-1}^*(\sigma, A, \theta) := P(X_{-1}(t) < 1, 0 \leq t \leq \theta/2 - s^*).$$

The sufficient condition for regular oscillations of the solution to (4.3)-(4.4) consists in the closeness of the probability $q_{-1,1}^* = 1 - p_{1,-1}^*$ to 1. To find $q_{-1,1}^*$ consider the following parabolic boundary value problem

$$\frac{\partial u}{\partial s} + \frac{\sigma^2}{2} \gamma(x) \frac{\partial^2 u}{\partial^2 x} + (x - x^3 + A) \frac{\partial u}{\partial x} = 0, \quad 0 \leq s < \theta/2 - s^*, \quad x < 1, \quad (4.5)$$

$$u(\theta/2 - s^*, x) = 0, \quad x < 1,$$

$$u(s, 1) = 1, \quad 0 \leq s \leq \theta/2 - s^*. \quad (4.6)$$

By the same arguments as in Section 2, it is not difficult to see that $q_{-1,1}^* = u(0, -1)$.

In the case of (4.3)-(4.4) the regular oscillations are observed under a more wide set of parameters than for (1.4)-(1.5) but under a more restricted set of parameters than for (4.1)-(4.2). Figure 4.4 shows a typical trajectory of the solution to (4.3)-(4.4) under values of parameters such that they do not ensure the regular oscillations in the case of the model (1.4)-(1.5). In Appendix see a numerical algorithm used here.

Remark 4.1. Using the approach proposed in Section 2, one can obtain a sufficient condition for regular oscillations in the system (1.3) which has an asymmetrical

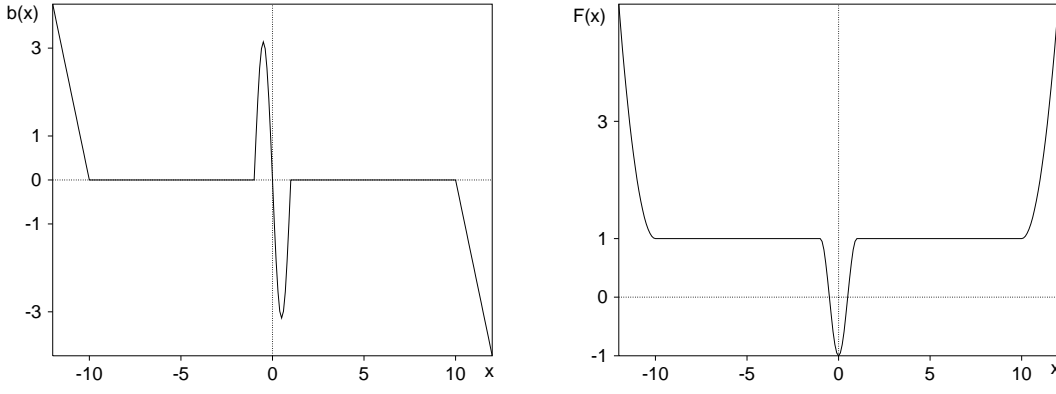


FIGURE 5.1. The function $b(x)$ of (5.2) and the potential $F(x)$ under $\alpha = 1$, $\beta = 10$, $\gamma = 1$.

bistable potential under some values of parameters (see [1]). Let the system (1.3) have two stable points x_- and x_+ , $x_- < x_+$, and one unstable x_u , $x_- < x_u < x_+$, in the absence of periodic forcing and noise. To give a sufficient condition for the regular oscillations in the asymmetrical case, four probabilities have to be considered: the probability q_{x_-,x_+} with which the trajectory starting from $x = x_-$ reaches the point $x = x_+$ during the first half-period of the periodic forcing (i.e., when the periodic forcing is positive); the probability p_{x_+,x_u} of unattainability of the point $x = x_u$ during the first half-period by the trajectory starting from $x = x_+$; the probability q_{x_+,x_-} with which the trajectory starting from $x = x_+$ reaches the point $x = x_-$ during the second half-period of the periodic forcing; the probability p_{x_-,x_u} of unattainability of the point $x = x_u$ during the second half-period by the trajectory starting from $x = x_-$. Due to the asymmetry, $q_{x_-,x_+} \neq q_{x_+,x_-}$ and $p_{x_+,x_u} \neq p_{x_-,x_u}$. In this situation, the sufficient condition of regular oscillations consists in the closeness of $q_{x_-,x_+} \cdot p_{x_+,x_u}$ and $q_{x_+,x_-} \cdot p_{x_-,x_u}$ to 1. One can easily write down boundary value problems for these probabilities.

5. Large-amplitude regular oscillations in monostable system

Consider the stochastic differential equation

$$dX = b(X)dt + A\chi(t; \theta)dt + \sigma dw, \quad (5.1)$$

where $\chi(t; \theta)$ is the θ -periodic function from (1.5),

$$b(x) = \begin{cases} -2\alpha(x + \beta), & x < -\beta, \\ -\gamma\pi \sin \pi x, & |x| < 1, \\ 0, & 1 \leq |x| \leq \beta, \\ -2\alpha(x - \beta), & x > \beta, \end{cases} \quad (5.2)$$

and $\alpha, \beta, \gamma > 0$ are some constants. See graphics of $b(x)$ and its potential $F(x) = -\int b(x)dx$ on Figure 5.1.

Under $A = 0$, $\sigma = 0$ the solution to (5.1) has the unique globally stable point $x = 0$. If $\sigma = 0$ and A is not large, the equation (5.1) has a θ -periodic solution with the amplitude less than 1 (see Figure 5.2a). After adding the noise of a certain level, the system does not exhibit regular oscillations (see Figure 5.2b). But an increase of the noise intensity leads to regular oscillations with large amplitude approximately equal to β (see Figure 5.2c).

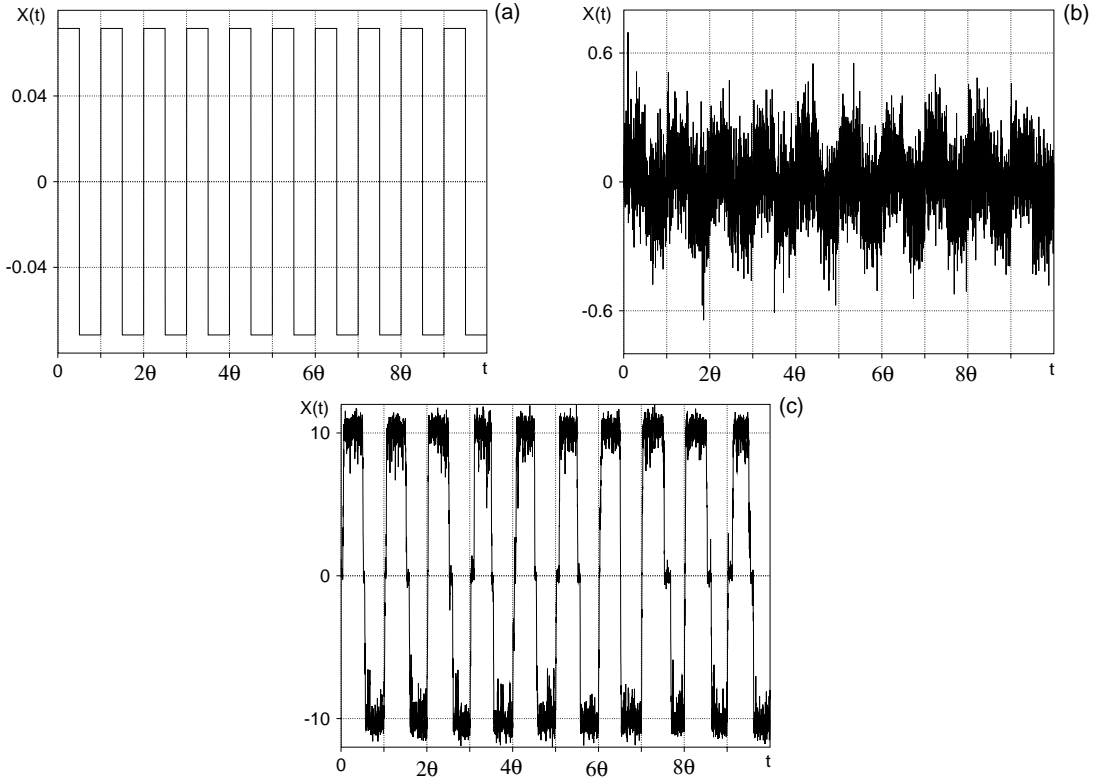


FIGURE 5.2. Sample trajectories of the solution to (5.1) under $\alpha = 1$, $\beta = 10$, $\gamma = 1$, $A = 0.7$, $\theta \approx 628.32$ ($\nu = 0.01$), and various σ : (a) $\sigma = 0$, (b) $\sigma = 0.55$, and (c) $\sigma = 1$.

To find a set of parameters under which the regular oscillations with large amplitude are observed, one can use the approach of Section 2 again. Introduce the probabilities

$$q_{-\beta,\beta} := 1 - P(X_{-\beta}(t) < \beta, 0 \leq t \leq \theta/2),$$

$$p_{\beta,1} := P(X_{\beta}(t) > 1, 0 \leq t \leq \theta/2).$$

Then the sufficient condition for the regular oscillations with amplitude β consists in the closeness of the product $q_{-\beta,\beta} \cdot p_{\beta,1}$ to 1. It is not difficult to write down the boundary value problems for calculating these probabilities just as in Section 2.

In [25] SR is observed in another monostable system.

6. Regular oscillations in system of two coupled oscillators

In this section we apply the proposed above approach to the system of two mutually coupled bistable overdamped oscillators

$$\begin{aligned} dX^1 &= (\alpha_1 X^1 - (X^1)^3)dt + c \cdot (X^2 - X^1)dt + A\chi(t; \theta)dt + \sigma dw_1(t) \\ dX^2 &= (\alpha_2 X^2 - (X^2)^3)dt + c \cdot (X^1 - X^2)dt + A\chi(t; \theta)dt + \sigma dw_2(t), \end{aligned} \tag{6.1}$$

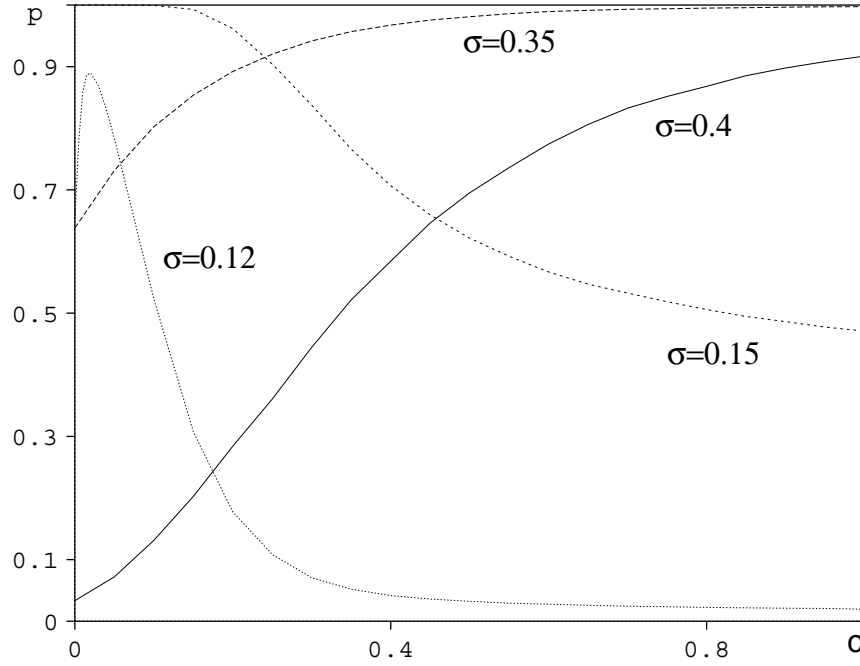


FIGURE 6.1. Two coupled oscillators. Dependence of the product $p(A, \sigma, \theta, c)$ in c under $A = 0.28$, $\theta = 10^4/3$, $\alpha_1 = \alpha_2 = 1$, and various σ .

where $w_1(t)$ and $w_2(t)$ are independent standard Wiener processes, the function $\chi(t; \theta)$ is defined in (1.5), the coefficients α_1 and α_2 , the strength of coupling c , and the noise intensity σ are some non-negative constants.

SR in a system similar to (6.1) was considered in [21]. The authors of [21] came to the conclusion that the maximum of the signal-to-noise ratio taken over noise intensity is a nonmonotonous function of coupling.

Here we are interested in the regular oscillations. Introduce the notation: $x_- = (-1, -1)$, $x_+ = (1, 1)$, $x_u = (0, 0)$ are the points belonging to R^2 , $X_x(t)$ is the solution of the system (6.1) which starts at the zero instant from the point $x \in R^2$,

$$p_{x_-, x_+} = p_{x_-, x_+}(A, \theta, \sigma, c) := P(X_{x_-}(t) \in R^2 \setminus \{x^1 > 1, x^2 > 1\}, 0 \leq t \leq \theta/2),$$

$$p_{x_+, x_u} = p_{x_+, x_u}(A, \theta, \sigma, c) := P(X_{x_+}(t) \in \{x^1 > 0, x^2 > 0\}, 0 \leq t \leq \theta/2),$$

and

$$q_{x_-, x_+} := 1 - p_{x_-, x_+}.$$

The sufficient condition of regular oscillations consists in the closeness of the product $p(A, \theta, \sigma, c) := q_{x_-, x_+} \cdot p_{x_+, x_u}$ to 1.

It is not difficult to write down the boundary value problems for calculating the probabilities q_{x_-, x_+} and p_{x_+, x_u} analogously to (2.9)-(2.10) and (2.12)-(2.13). Solving these problems numerically, we find the product p which bounds the probability of regular oscillations from below. Figures 6.1, 6.2, and 6.3 present results of our calculations of p . One can see that an increase of coupling leads to shift of the domain of parameters corresponding to regular oscillations. The domain is shifted to the range of larger noise intensities (see Figures 6.2 and 6.3). An increase of

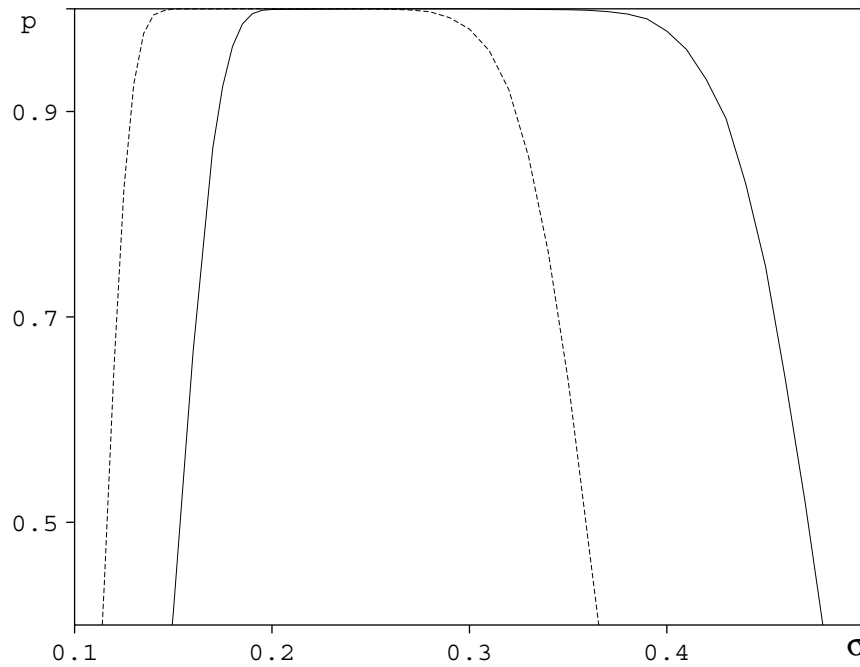


FIGURE 6.2. Two coupled oscillators. Dependence of the product $p(A, \sigma, \theta, c)$ in σ under $A = 0.28$, $\theta = 10^4/3$, $\alpha_1 = \alpha_2 = 1$, and $c = 0$ (dashed line), $c = 2$ (solid line).

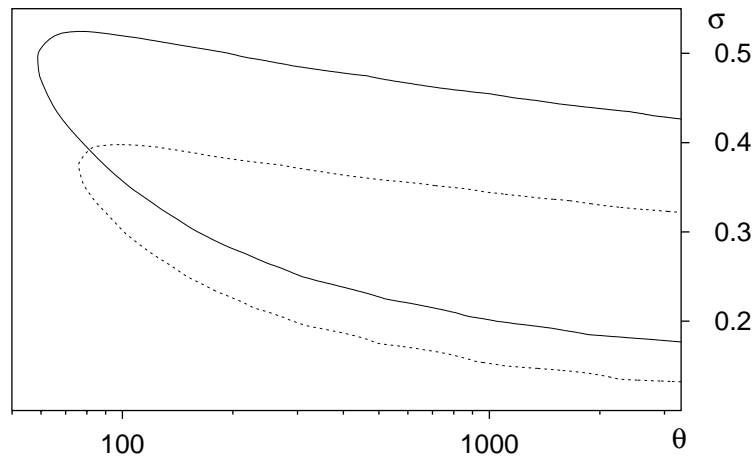


FIGURE 6.3. Two coupled oscillators. Curves of the level 0.9 of the product $p(A, \sigma, \theta, c)$ in the plane (θ, σ) under $A = 0.28$ and various c : $c = 0$ (dashed line) and $c = 2$ (solid line); θ in the logarithmic scale.

the coupling can both decrease and increase the product p depending on the taken A, σ, θ (see Figure 6.1).

Figures 6.4 and 6.5 show typical trajectories of the first oscillator under various collections of the parameters. Figure 6.4 demonstrates that for some fixed A, σ, θ

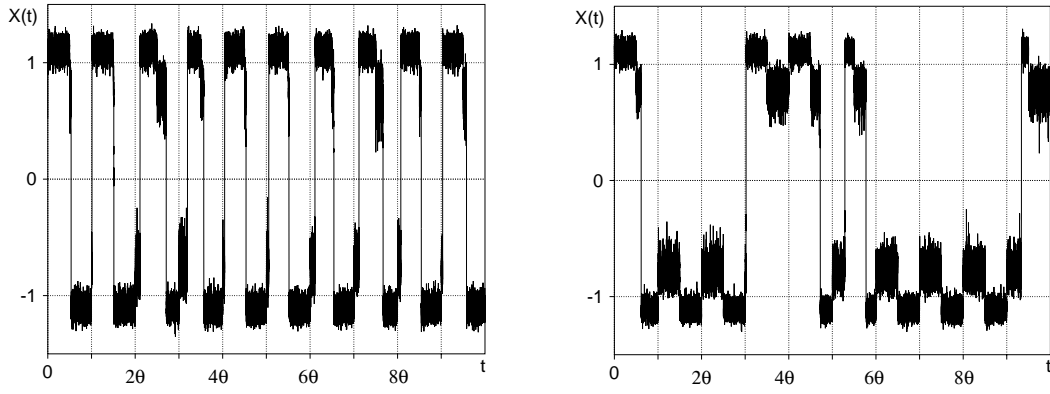


FIGURE 6.4. Two coupled oscillators. Sample trajectories of the first oscillator under $A = 0.28$, $\theta = 10^4/3$, $\sigma = 0.15$, $\alpha_1 = \alpha_2 = 1$, and various c : $c = 0$ (left) and $c = 2$ (right).

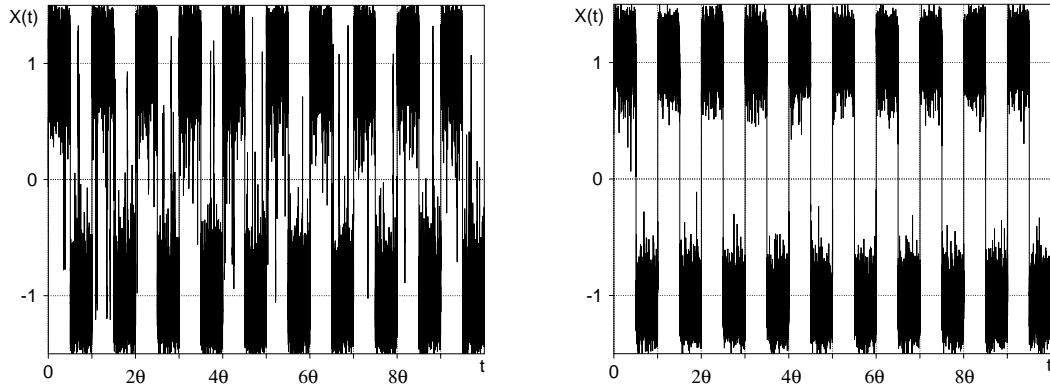


FIGURE 6.5. Two coupled oscillators. Sample trajectories of the first oscillator under $\sigma = 0.45$ and various c : $c = 0$ (left) and $c = 3$ (right). Other parameter values are the same as in Figure 6.4.

disappearance of regular oscillations for (6.1) can result from an increase of coupling c . And vice versa, Figure 6.5 presents the situation when an increase of coupling leads to existence of the regular oscillations.

7. Appendix. The used numerical algorithms

7.1. Probabilistic methods for solving boundary value problems. Probabilistic methods for boundary value problems are based on probabilistic representations of their solutions. The representations are connected with systems of SDE. To realize them, Markov chains which weakly approximate the solutions of these systems are constructed. Unlike usual approximations of SDE, when a time discretization is exploited, space (for elliptic problems) and space-time (for parabolic problems) discretizations are recommended in the case of boundary value problems (see [16, 17]). This kind of discretization allows one to ensure that the constructed Markov chains belong to the bounded domain associated with a considered boundary value problem.

As an example, let us give a probabilistic method in application to the problem (2.9)-(2.10). The solution $u(t, x)$ has the probabilistic representation

$$u(t, x) = E\varphi(\vartheta_{t,x}, X_{t,x}(\vartheta_{t,x})), \quad (7.1)$$

where

$$\varphi(t, x) = \begin{cases} 0, & t = \theta/2, x < 1, \\ 1, & 0 \leq t \leq \theta/2, x = 1, \end{cases}$$

$X_{t,x}(s)$, $s \geq t$, satisfies the SDE

$$dX = (X - X^3 + A)ds + \sigma dw(s), \quad X(t) = x < 1, \quad (7.2)$$

and $(\vartheta_{t,x}, X_{t,x}(\vartheta_{t,x}))$ is the first exit point of the space-time diffusion $(s, X_{t,x}(s))$, $s > t$, to the boundary Γ of the domain $Q = [0, \theta/2) \times (-\infty, 1)$. Note that the boundary Γ consists of $\{\theta/2\} \times (-\infty, 1) \cup [0, \theta/2] \times \{1\}$.

To avoid any misunderstanding, we observe that the representation (7.1) is distinguished from (2.8) only in form and $\vartheta_{t,x} = \tau_{t,x} \wedge \theta/2$.

Introduce the neighborhood $\Gamma_\delta \in Q$ of the boundary Γ : $\Gamma_\delta = [\theta/2 - \delta, \theta/2) \times (-\infty, 1) \cup [0, \theta/2) \times [1 - \delta, 1)$. Consider the Markov chain (t_k, X_k) , $t_0 = t$, $X_0 = x$, which weakly approximates the points $(t_k, X_{t,x}(t_k))$ of the trajectory $(s, X_{t,x}(s))$.

Due to one of the probabilistic methods from [16], the recurrence sequence (t_k, X_k) can be constructed in the following way:

$$t_0 = t, \quad X_0 = x,$$

$$t_{k+1} = t_k + r_k^2,$$

$$X_{k+1} = X_k + \sigma r_k \eta_k + r_k^2 \cdot (X_k - X_k^3 + A) + \sigma r_k^3 \cdot (1 - 3X_k^2) \eta_k / 2$$

$$+ r_k^4 [(X_k - X_k^3 + A)(1 - 3X_k^2) - 3\sigma^2 X_k] / 2,$$

$$k = 0, 1, 2, \dots,$$

where η_k are i.i.d. random variables with the law $P(\eta = 0) = 2/3$, $P(\eta = \pm\sqrt{3}) = 1/6$ and the sequence r_k is constructed so that (t_k, X_k) belongs to \overline{Q} at every step k .

Let $r > 0$ and $c = \sqrt{3}\sigma + \max(\sqrt{3}\sigma, r \cdot (2\sqrt{3} + A))$. If $(t_k, X_k) \in Q \setminus \Gamma_{cr}$, we put $r_k = r$. One can check that if $(t_k, X_k) \in Q \setminus \Gamma_{cr}$ and r is sufficiently small, then $(t_{k+1}, X_{k+1}) \in \overline{Q}$. If $(t_k, X_k) \in \Gamma_{cr}$ and $\rho_k := 1 - X_k \leq cr$, then $|X_{k+1} - X_k| \leq \sqrt{3}\sigma r_k + Cr_k^2$, $C = A + 2cr$, and $1 - X_{k+1} \leq \rho_k - \sqrt{3}\sigma r_k - Cr_k^2$. So, if $(t_k, X_k) \in \Gamma_{cr}$, to ensure $(t_{k+1}, X_{k+1}) \in \overline{Q}$ we put $r_k = \min(\rho_k / (\sqrt{3}\sigma + C\rho_k / (\sqrt{3}\sigma)), \sqrt{\theta/2 - t_k})$.

We stop the Markov chain (t_k, X_k) at a step \varkappa when the chain exits from the domain $Q \setminus \Gamma_{r^4}$. Then we find the point $(\bar{t}_\varkappa, \bar{X}_\varkappa)$ on the boundary Γ which is close to $(t_\varkappa, X_\varkappa)$: if $\theta/2 - t_k \leq r^4$, we put $\bar{t}_\varkappa = \theta/2$, $\bar{X}_\varkappa = X_\varkappa$ and otherwise $\bar{t}_\varkappa = t_\varkappa$, $\bar{X}_\varkappa = 1$. As it is proved in [16], the point $(\bar{t}_\varkappa, \bar{X}_\varkappa)$ approximates weakly the point $(\vartheta_{t,x}, X_{t,x}(\vartheta_{t,x}))$ with the error estimated by $O(r^4)$. The mean value $E\varkappa$ of number of steps is estimated by $O(r^2)$.

Now we are able to approximate the expectation in (7.1):

$$u(t, x) = E\varphi(\vartheta_{t,x}, X_{t,x}(\vartheta_{t,x})) \doteq E\varphi(\bar{t}_\varkappa, \bar{X}_\varkappa) := \bar{u}(t, x). \quad (7.3)$$

Due to results of [16]

$$|u(t, x) - \bar{u}(t, x)| \leq Kr^4.$$

To evaluate the mean value in the right-hand side of (7.3), the Monte Carlo procedure is used

$$E\varphi(\bar{t}_\varkappa, \bar{X}_\varkappa) \doteq \frac{1}{N} \sum_{n=1}^N \varphi(\bar{t}_\varkappa^{(n)}, \bar{X}_\varkappa^{(n)}) := \bar{\bar{u}}(t, x),$$

where $(\bar{t}_\varkappa^{(n)}, \bar{X}_\varkappa^{(n)})$, $n = 1, \dots, N$, are independent realizations of $(\bar{t}_\varkappa, \bar{X}_\varkappa)$, and the Monte Carlo error is estimated by

$$err_{MC} = \frac{2}{\sqrt{N}} \left(\frac{1}{N} \sum_{n=1}^N \varphi^2(\bar{t}_\varkappa^{(n)}, \bar{X}_\varkappa^{(n)}) - (\bar{\bar{u}}(t, x))^2 \right)^{1/2}.$$

Taking into account that $\varphi(t, x)$ takes the values 0 and 1 only, we get

$$err_{MC} = \frac{2}{\sqrt{N}} (\bar{\bar{u}}(t, x)(1 - \bar{\bar{u}}(t, x)))^{1/2}.$$

Hence, if $\bar{\bar{u}}(t, x)$ is close to 0 or to 1, the Monte Carlo error is small and we can take not too large N to reach a fairly high exactness. Note that to get a domain of parameters corresponding to the regular oscillations, we are mainly interested in accurate simulation of $u(t, x)$, when its value is fortunately close to 1.

Throughout our numerical experiments we use a generator of uniform random numbers from [23]. We usually take $r = \sqrt{2} \cdot 10^{-1}$ and $N = 10000$.

In the one-dimensional case probabilistic algorithms require computational effort similar to finite-difference schemes. But the Monte Carlo approach is more effective under space dimension greater than 1.

When the value of σ is sufficiently small, it is preferable to attract weak numerical methods of [19]. These methods are specially intended to approximate (in the weak sense) solutions of SDE with small noise and are highly efficient. In [26] the special methods of [19] were effectively applied to evaluation of the signal-to-noise ratio in systems with SR.

7.2. Mean-square methods for simulating sample trajectories of SDE. To simulate sample trajectories of SDE, one has to use mean-square methods [15]. In our experiments we mainly use the mean-square Euler scheme. In the case of the SDE (1.4) it takes the form

$$X_x(t_{k+1}) \approx X_{k+1} = X_k + h \cdot (X_k - X_k^3) + hA\chi(t_k; \theta) + \sigma h^{1/2} \xi_k, \quad X_0 = x,$$

where h is a step of time discretization, ξ_k are independent normally distributed random variables with zero mean and unit variance.

The global mean-square error of this scheme is estimated by $O(h)$. Because of discontinuity of $\chi(t; \theta)$, a time step h should be such that $\theta/2h$ is an integer.

Note that in the case of SDE with additive noise (1.4) the mean-square method with error $O(h^{3/2})$ [15], i.e., more accurate than the Euler scheme, can be applied. If the noise intensity σ is small, SR is observed under large θ and one should simulate the system on long time intervals. In this case the most preferable methods are ones of [18], where efficient high-exactness mean-square methods for SDE with small noise

are proposed. To use these special methods is essentially important if a system of high-dimension (e.g., an array of coupled oscillators [11]) is under consideration.

Now let us give a remark on simulation of SDE (4.1)-(4.2) and (4.3)-(4.4). If a model has discontinuous in time and continuous in space coefficients, there are no serious problems in its simulation. Despite the diffusion coefficient in (4.1)-(4.2) is discontinuous in t and x , principal difficulties do not arise as well. It is so because any trajectory of (4.1)-(4.2) feels the discontinuity of the diffusion coefficient in x not more than once during the half-period $\theta/2$. As to (4.3)-(4.4), discontinuity in x of the diffusion coefficient leads to some problems in numerical simulations. Indeed, if $X(t) \geq -1$ at a moment $t \in [n\theta, (n+1/2)\theta)$, $n = 0, 1, 2, \dots$, then $X(s) > -1$ for all $s \in (t, (n+1/2)\theta)$ with probability 1. But due to the discretization error the mean-square Euler approximation \tilde{X}_k of $X(t_k)$ violates this property and can become less than -1 . As a result, it gives a too distorted image of the real behavior. To overcome this difficulty, we propose a modified approximation \tilde{X}_k (agreeing with the above-mentioned property of trajectories):

$$\tilde{X}_0 = x, \quad t_0 = 0, \quad (7.4)$$

$$\hat{X}_{k+1} = \tilde{X}_k + h \cdot (\tilde{X}_k - \tilde{X}_k^3) + hA\chi(t_k; \theta) + h^{1/2}\sigma\xi_k;$$

$$\text{if } \tilde{X}_k < -1 \text{ or } \tilde{X}_k > 1, \text{ then } \tilde{X}_{k+1} = \hat{X}_{k+1};$$

$$\text{if } -1 \leq \tilde{X}_k \leq 1 \text{ and } \chi(t_k; \theta) > 0, \text{ then } \tilde{X}_{k+1} = \max(-1, \hat{X}_{k+1});$$

$$\text{if } -1 \leq \tilde{X}_k \leq 1 \text{ and } \chi(t_k; \theta) < 0, \text{ then } \tilde{X}_{k+1} = \min(\hat{X}_{k+1}, 1);$$

$$k = 0, 1, 2, \dots$$

Here h is a step of the time discretization, ξ_k are independent normally distributed random variables with zero mean and unit variance.

We also take the continuous $\gamma(x) = \arctan(\alpha(x-1)) + \arctan(-\alpha(x+1))$ instead of (4.4) and integrate (4.3) with this $\gamma(x)$ under a big α by the mean-square Euler method with a sufficiently small time step. Simulations with the continuous $\gamma(x)$ and simulations due to (7.4) demonstrate similar results.

The same difficulties arise for numerical solution of the boundary value problem (4.5)-(4.6). They can be overcome in a similar manner.

Acknowledgement

The second author is grateful to the Alexander von Humboldt Foundation for support of this work through a research fellowship.

REFERENCES

- [1] R. Bartussek, P. Hänggi, and P. Jung. *Stochastic resonance in optical bistable systems*. Phys. Rev. E, v. 49 (1994), pp. 3930-3939.
- [2] R. Benzi, G. Parisi, A. Suttera, and A. Vulpiani. *Stochastic resonance in climatic change*. Tellus, v. 34 (1982), pp. 10-16; R. Benzi, A. Suttera, and A. Vulpiani. *The mechanism of stochastic resonance*. J. Phys. A, v.14 (1981), pp. L453-L457.
- [3] M.I. Dykman, D.G. Luchinsky, P.V.E. McClintock, N.D. Stein, and N.G. Stocks. *Stochastic resonance for periodically modulated noise intensity*. Phys. Rev. A, v. 46 (1992), pp. R1713-R1716.

- [4] M.I. Dykman, D.G. Luchinsky, R. Mannella, P.V.E. McClintock, N.D. Stein, and N.G. Stocks. *Supernarrow spectral peaks and high-frequency stochastic resonance in systems with periodic attractors*. Phys. Rev. E, v. 49 (1994), pp. 1198-1204.
- [5] E.B. Dynkin. *Markov Processes*. (English translation in two volumes). Springer, Berlin, 1965.
- [6] L. Gammaitoni, P. Hänggi, P. Jung, and F. Marchesoni. *Stochastic resonance*. Rev. Mod. Phys., v. 70 (1998), pp. 223-287.
- [7] I.I. Gichman, A.V. Skorochod. *Stochastic Differential Equations*. Naukova Dumka, Kiev, 1968.
- [8] P. Hänggi and R. Bartussek. *Brownian rectifiers: How to covert Brownian motion into directed transport*. In "Nonlinear Physics of Complex Systems: current status and future trends." J. Parisi, S.C. Müller, and W. Zimmermann (Eds.), Lecture Notes in Physics, v. 476, Springer, 1996, pp. 294-308.
- [9] W. Horsthemke and R. Lefever. *Noise-Induced Transitions: Theory and Applications in Physics, Chemistry and Biology*. Springer, 1984.
- [10] F. Jülicher, A. Ajdari, and J. Prost. *Modeling molecular motors*. Rev. Mod. Phys., v. 69 (1997), pp. 1269-1281.
- [11] J.F. Lindner, B.K. Meadows, W.L. Ditto, M.E. Inchiosa, and A.R. Bulsara. *Array enhanced stochastic resonance and spatiotemporal synchronization*. Phys. Rev. Lett., v. 75 (1995), pp. 3-6.
- [12] M.O. Magnasco. *Forced thermal ratchets*. Phys. Rev. Lett., v. 71 (1993), pp. 1477-1481.
- [13] M.O. Magnasco. *Brownian combustion engines*. In "Fluctuations and Order: the new synthesis". M. Millonas (Ed.), Springer, 1996, pp. 307-320.
- [14] R. Mannella and P.V.E. McClintock, Eds. *Proceedings of the International Workshop "Fluctuations in Physics and Biology: Stochastic Resonance, Signal Processing and Related Phenomena"*. Nuovo Cimento Della Societa Italiana di Fisica D, v. 17 (1995), No 7/8.
- [15] G.N. Milstein. *Numerical Integration of Stochastic Differential Equations*. Ural Univ. Press, Sverdlovsk, 1988; Kluwer Academic Publishers, 1995.
- [16] G.N. Milstein. *Solving the first boundary value problem of parabolic type by numerical integration of stochastic differential equations*. Theory Prob. Appl., v. 40 (1995), pp. 657-665.
- [17] G.N. Milstein. *Weak approximation of a diffusion process in a bounded domain*. Stochastics and Stochastics Reports, v. 62 (1997), pp.147-200.
- [18] G.N. Milstein and M.V. Tretyakov. *Mean-square numerical methods for stochastic differential equations with small noises*. SIAM J. Sci. Comput., v. 18 (1997), pp. 1067-1087.
- [19] G.N. Milstein and M.V. Tretyakov. *Numerical methods in the weak sense for stochastic differential equations with small noise*. SIAM J. Numer. Anal., v. 34 (1997), pp. 2142-2167.
- [20] F. Moss. *Stochastic resonance: From the ice ages to the monkey's ear*. In "Contemporary problems in statistical physics". G.H.Weiss (Ed.), SIAM, Philadelphia, 1994, pp. 205-253.
- [21] A. Neiman and L. Schimansky-Geier. *Stochastic resonance in two coupled bistable systems*. Phys. Lett. A, v. 197 (1995), pp. 379-386.
- [22] C. Nicolis. *Stochastic aspects of climatic transitions - response to a periodic forcing*. Tellus, v. 34 (1982), pp. 1-9.
- [23] W.H. Press, S.A. Teukolsky, W.T. Vetterling, and B.P. Flannery. *Numerical Recipes in C: The Art of Scientific Computing*. Cambridge Univ. Press, Cambridge, 1992.
- [24] L. Schimansky-Geier and Th. Pöschel, Eds. *Stochastic Dynamics*. Lecture Notes in Physics, v. 484, Springer, 1997.
- [25] N.G. Stocks, N.D. Stein, and P.V.E. McClintock. *Stochastic resonance in monostable systems*. J. Phys. A, v. 26 (1993), pp. L385-L390.
- [26] M.V. Tretyakov. *Numerical technique for studying stochastic resonance*. Phys. Rev. E, v. 57 (1998), pp. 4789-4794.